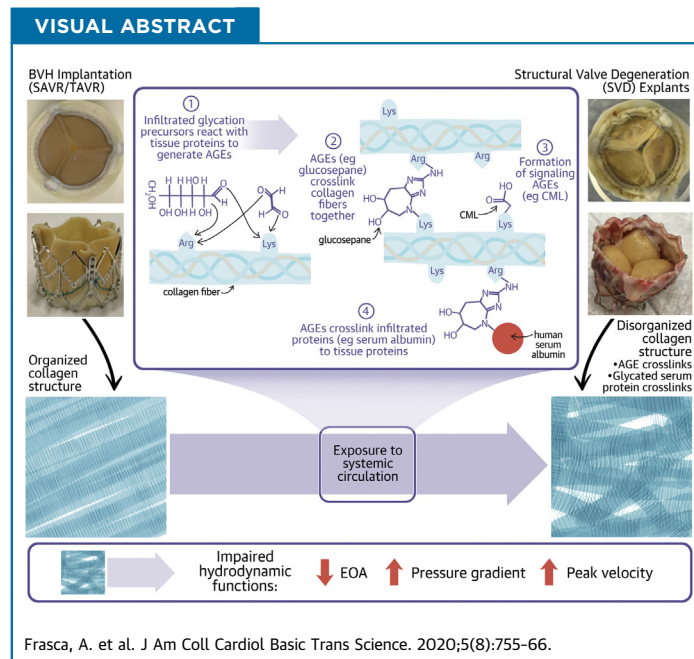


CLINICAL RESEARCH

Glycation and Serum Albumin Infiltration Contribute to the Structural Degeneration of Bioprosthetic Heart Valves



Antonio Frasca, PhD,^a Yingfei Xue, PhD,^a Alexander P. Kossar, MD,^a Samuel Keeney, BS,^b Christopher Rock, PhD,^b Andrey Zakharchenko, PhD,^b Matthew Streeter, PhD,^c Robert C. Gorman, MD,^d Juan B. Grau, MD,^e Isaac George, MD,^a Joseph E. Bavaria, MD,^d Abba Krieger, PhD,^d David A. Spiegel, PhD,^c Robert J. Levy, MD,^b Giovanni Ferrari, PhD^a



From the ^aDepartment of Surgery, Columbia University, New York, New York; ^bDepartment of Pediatrics, The Children's Hospital of Philadelphia, Philadelphia, Pennsylvania; ^cDepartment of Chemistry, Yale University, New Haven, Connecticut; ^dDepartment of Surgery, University of Pennsylvania, Philadelphia, Pennsylvania; and the ^eOttawa Heart Institute, Ottawa, Ontario, Canada. This work was supported by National Institutes of Health grants R01s HL122805 (to Dr. Ferrari) and HL143008 (to Drs. Levy and Ferrari), T32s HL007915 (to Drs. Levy and Rock), HL007854 (to Dr. Kossar) and HL007343 (to Dr. Frasca), The Kibel Fund for Aortic Valve Research (to Drs. Ferrari and Levy), The Valley Hospital Foundation 'Marjorie C Bunnel' charitable fund (to Drs. Ferrari and Grau), the American Diabetes Association Pathway to Stop Diabetes Grant 1-17-VSN-04 and the SENS Research Foundation (to Dr. Spiegel), and both Erin's Fund and the William J Rashkind Endowment of the Children's Hospital of Philadelphia (to Dr. Levy). Dr. Spiegel is cofounder and chief scientific adviser at REVEL Pharmaceuticals. Dr. Levy is a consultant for WL Gore. All other authors have reported that they have no relationships relevant to the contents of this paper to disclose. The authors attest they are in compliance with human studies committees and animal welfare regulations of the authors' institutions and Food and Drug Administration guidelines, including patient consent where appropriate. For more information, visit the *JACC: Basic to Translational Science* [author instructions page](#).

Manuscript received March 24, 2020; revised manuscript received June 2, 2020, accepted June 2, 2020.

**ABBREVIATIONS
AND ACRONYMS****AGE** = advanced glycation end product**BHV** = bioprosthetic heart valve**BP** = bovine pericardium**CML** = *N*-carboxymethyl-lysine**EOA** = effective orifice area**HSA** = human serum albumin**IHC** = immunohistochemistry**PBS** = phosphate-buffered saline**SAVR** = surgical aortic valve replacement**SHG** = second harmonic generation**SVD** = structural valve degeneration**TAVR** = transcatheter aortic valve replacement**HIGHLIGHTS**

- **Two novel and interacting mechanisms contributing to BHV SVD are reported: glycation and serum albumin infiltration.**
- **Glycation product formation and serum albumin deposition were observed in 45 clinical BHV explanted due to SVD as well as BHV tissue subcutaneously implanted in rats.**
- **In vitro exposure to glycation and serum albumin elicited collagen network misalignment similar to that seen in clinical and rat explant BHV tissue.**
- **Glycation was sufficient to impair BHV hydrodynamic function in ISO-5840-compliant pulse duplication testing and concomitant serum albumin infiltration exacerbated these effects.**

SUMMARY

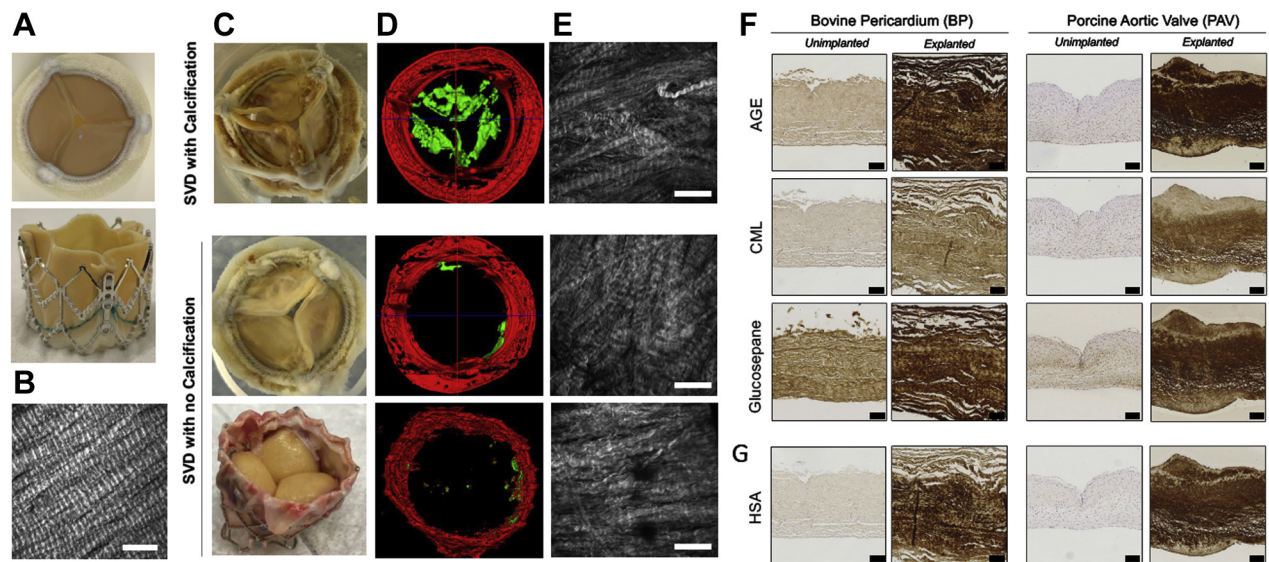
Valvular heart diseases are associated with significant cardiovascular morbidity and mortality, and often require surgical and/or percutaneous repair or replacement. Valve replacement is limited to mechanical and biological prostheses, the latter of which circumvent the need for lifelong anticoagulation but are subject to structural valve degeneration (SVD) and failure. Although calcification is heavily studied, noncalcific SVD, which represent roughly 30% of BHV failures, is relatively underinvestigated. This original work establishes 2 novel and interacting mechanisms—glycation and serum albumin incorporation—that occur in clinical valves and are sufficient to induce hallmarks of structural degeneration as well as functional deterioration. (J Am Coll Cardiol Basic Trans Science 2020;5:755-66) © 2020 The Authors. Published by Elsevier on behalf of the American College of Cardiology Foundation. This is an open access article under the CC BY-NC-ND license (<http://creativecommons.org/licenses/by-nc-nd/4.0/>).

Bioprosthetic heart valves (BHVs) are widely used to treat heart valve disease. BHV leaflets are fabricated from glutaraldehyde cross-linked heterografts—predominantly bovine pericardium (BP) or porcine aortic valves. BHV are preferred over mechanical valves due to their technical versatility, adaptability to transcatheter valvular approaches, and freedom from lifelong anticoagulation therapy (1-3). However, BHVs are limited by degeneration of leaflet tissue matrix, termed “structural valve degeneration” (SVD). SVD, whose definition has recently been standardized (3), constitutes pathological modification of valve leaflets ultimately compromising biomechanical function. SVD occurs in all BHV recipients and is exacerbated in certain subpopulations, including patients with diabetes (4) and younger patients (5,6). BHV lifespans are limited by SVD (3,7) to an average of between 10 and 15 years. This process is driven by cellular, biochemical, and biomechanical mechanisms arising from valve properties, patient characteristics, and the interactions between them. Calcification is observed in the majority of SVD cases; however, approximately 30% of SVD cases are not associated with significant calcification (8,9). Further, observation suggests that calcification might be associated with SVD without necessarily being functionally causative (8). Several noncalcific mechanisms have

been proposed to contribute to SVD, including inflammatory oxidation, tissue thickening, and collagen network degeneration (7,10); however, technologies to address known mechanisms thus far have not significantly improved valve durability, suggesting that additional key mechanisms remain unidentified (6).

Glycation is a complex constellation of nonenzymatic biochemical reactions involving the adduction of sugar-derived moieties to protein nucleophilic groups. Glycation may involve biologically significant intermediates, such as Amadori products, and culminates in the formation of biologically irreversible advanced glycation end products (AGEs) (11-13). Glycation strongly contributes to structural and functional degeneration in various native tissues and diseases via 2 major avenues: 1) direct modification of extracellular matrix proteins via crosslinking and modification of protein interactions; and 2) modulation of cell phenotypes and instigation of inflammation via glycation product-mediated receptor signaling (14,15). Glycation elicits degeneration of collagenous native tissues via crosslinking and resultant disruption of collagen networks (16-18); yet, it has not been considered in the pathophysiology of BHV leaflets, for which collagen type I is the majority component (19,20). BHV lack living native cells or a functional surface barrier. Glycation in this context is

FIGURE 1 Glycation and HSA Infiltration in Clinical SVD



(A) Visuals of unimplanted surgical (Edwards PERIMOUNT, **top**) and transcatheter (Edwards SAPIEN XT [Edwards Lifesciences], **bottom**) BHV. **(B)** SHG image of unimplanted BHV tissue (scale = 100 μ m). **(C)** Visuals of failed clinical surgical aortic valve replacement (**top and middle**) and transcatheter aortic valve replacement (**bottom**) valves. **(D)** Micro-computed tomography scans and **(E)** SHG images of calcified (**top row**) and noncalcified (**middle and bottom rows**) failed BHV (scale = 100 μ m). **(F)** IHC for generalized AGE, CML, and glucosepane in 2 representative failed clinical BHV alongside unimplanted BHV tissue for both bovine pericardium and porcine aortic valve BHV (scale = 100 μ m). **(G)** IHC for HSA on the same samples as **F**. AGE = advanced glycation end product; BHV = bioprosthetic heart valve; CML = N-carboxymethyl-lysine; HSA = human serum albumin; IHC = immunohistochemistry; SHG = second harmonic generation; SVD = structural valve degeneration.

likely to occur primarily via infiltration from the surrounding blood of: 1) glycation precursors that modify the extracellular matrix structure directly; 2) pre-glycated proteins that deposit in BHVs; and 3) nonglycated proteins that are glycosylated in situ by infiltrated precursors. Therefore, we hypothesized that glycation and infiltration by human serum albumin (HSA), the most abundant and glycation-susceptible circulating protein (21,22), synergistically contribute to BHV SVD.

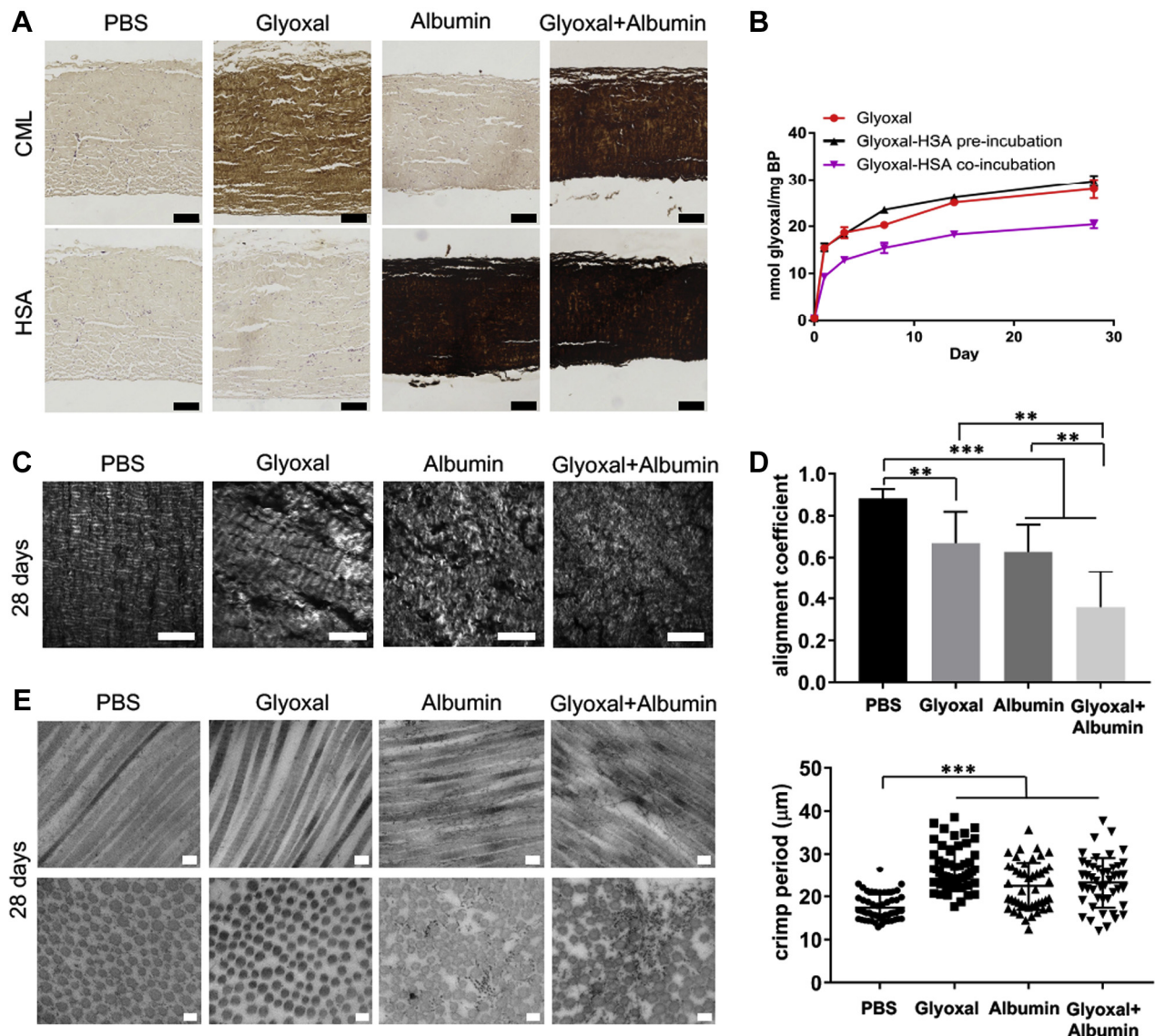
METHODS

PATIENT POPULATION. In order to establish clinical relevance for glycation and albumin infiltration in BHV, 45 patients with BHV aortic valve replacements requiring reoperation and BHV explantation were studied (Supplemental Table 1). Endocarditis was excluded. At initial operation, 25 patients (55.6%) underwent valve replacement only, 6 (13.3%) underwent valve replacement with aortic root replacement, 2 (4.4%) underwent valve replacement with ascending aorta repair, 2 (4.4%) underwent valve replacement concomitantly with coronary artery bypass grafting, and 10 (22.2%) underwent aortic

valve replacement concomitantly with mitral valve repair. BHV durations ranged from 3.5 to 14.8 years (mean duration 8.6 ± 0.4 years). Echocardiography preceding reoperation demonstrated BHV aortic insufficiency in 33 patients (73.3%) and BHV aortic stenosis in 37 patients (82.2%). Comorbidities included aortic dilatation (26.7%), diabetes (17.8%), coronary artery disease (40.0%), hyperlipidemia (46.7%), hypertension (73.3%), smoking (33.3%), and bicuspid aortic valve (42.2%). Nearly one-half of patients (44.4%) had been treated with statins.

IN VITRO GLYCATION/SERUM ALBUMIN EXPOSURE. In order to model glycation and albumin infiltration in BHV tissue in vitro, 8-mm biopsy punches of BP were incubated in phosphate-buffered saline (PBS) (Corning, Corning, New York), PBS + 5% clinical-grade HSA (from stock 25% HSA, Octapharma via NOVA Biologics, Oceanside, California), PBS + 50 mmol/l glyoxal (from stock 88 mol/l glyoxal, Sigma-Aldrich, St. Louis, Missouri), or PBS + 50 mmol/l glyoxal + 5% serum albumin for 24 h, 2 weeks, or 4 weeks at 37°C.

RAT SUBCUTANEOUS MODEL. In order to model glycation and albumin infiltration in BHV tissue

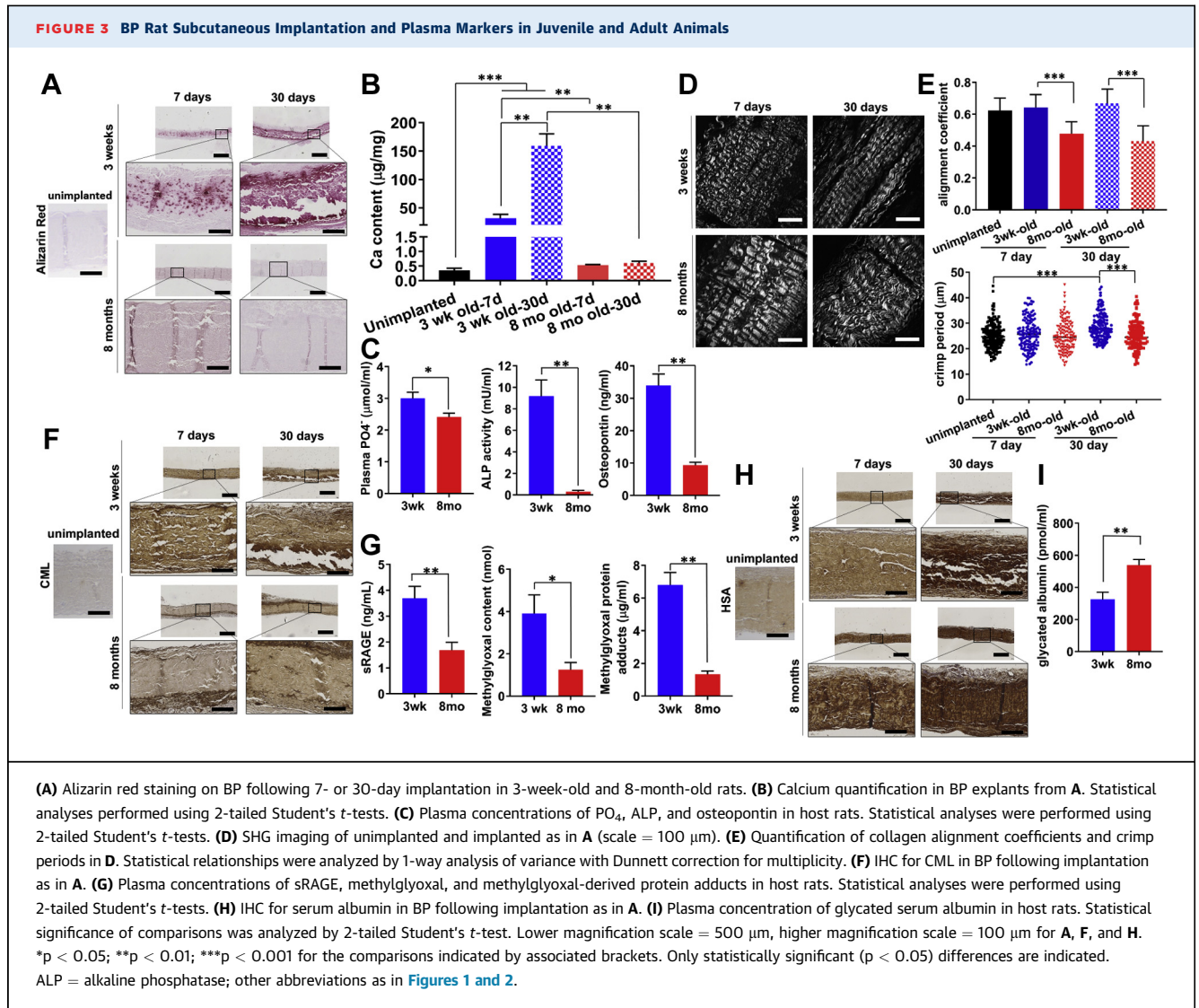
FIGURE 2 In Vitro Modeling of BHV Interactions With Glyoxal and HSA

(A) IHC for CML and HSA in cross sections of BP incubated with glyoxal and/or HSA for 24 h at 37°C (scale = 100 μm). (B) Line plot of ¹⁴C-glyoxal uptake by BP. (C) SHG imaging of BP (scale = 100 μm). (D) Quantifications of collagen fiber alignment coefficient (top) and collagen crimp period (bottom) in C. Statistical relationships were analyzed by 1-way analysis of variance with Dunnett correction for multiplicity. *p < 0.05; **p < 0.01; ***p < 0.001 for the comparisons indicated by associated brackets. Only statistically significant (p < 0.05) differences are indicated. (E) Transmission electron micrographs of longitudinal (top row) and cross-sectional (bottom row) views of collagen fibers in BP. BP = bovine pericardium; PBS = phosphate-buffered saline; other abbreviations as in Figure 1.

in vivo, 8- to 10-mm discs of BP were subcutaneously implanted in 3-week-old Sprague-Dawley rats (n = 26; Charles River Laboratories, Wilmington, Massachusetts), with adherence to an approved protocol (AAAR6796). Each animal received 1 implant per subcutaneous pocket, with 4 to 6 implants per animal. Blood was drawn at the time of animal sacrifice via cardiac puncture and collected in EDTA blood

tubes, after which it was immediately centrifuged at 4°C and 1,000 relative centrifugal force for 15 min. Plasma was aliquoted and stored at -80°C.

PULSE DUPLICATION. In order to evaluate the functional effects of glycation and concomitant albumin infiltration in BHV, hydrodynamic pulsatile functionality of BHV was tested on a commercial, ISO 5840-compliant pulse duplicator (HDTI-6000, BDC



Laboratories, Wheat Ridge, Colorado) with a PD-1100 pulsatile pump (BDC Laboratories). The flow, pulse rate, and driving waveform shape were controlled through Statys software (version 1.2) (BDC Laboratories). The pressure was adjusted via the Systemic Mean Pressure Control knob. Detailed experiment setup and calculation of all relevant parameters are described in the [Supplemental Appendix](#).

RESULTS

CALCIFICATION, COLLAGEN MALALIGNMENT, GLYCATION, AND HSA INFILTRATION IN EXPLANTED BHV ARE ASSOCIATED WITH SVD. With institutional review board approval (AAAR6796 [Columbia University] and 809349 [University of Pennsylvania]), surgical aortic valve replacement (SAVR)

bioprosthetic explants were retrieved for this study (*n* = 45) from patients ranging in age from 34 to 86 years at the time of reoperation (mean 65.0 ± 13.6 years) ([Supplemental Table 1](#), [Supplemental Methods](#)). A transcatheter aortic valve replacement (TAVR) bioprosthesis was also obtained and analyzed.

Calcification results ([Supplemental Figure 1](#)) showed an average leaflet calcification of 126 µg of calcium/mg of leaflet mass (SD = 107 µg/mg). Thirteen valves exhibited nearly no calcification (<10 µg/mg), 6 valves had intermediate calcification (between 10 and 100 µg/mg), and 26 valves had high calcification (>100 µg/mg). Unimplanted BHV were characterized with second-harmonic generation (SHG) microscopy, which demonstrated organized alignment of collagen fiber bundles ([Figures 1A and 1B](#)). Representative micro-computed tomography and SHG images of

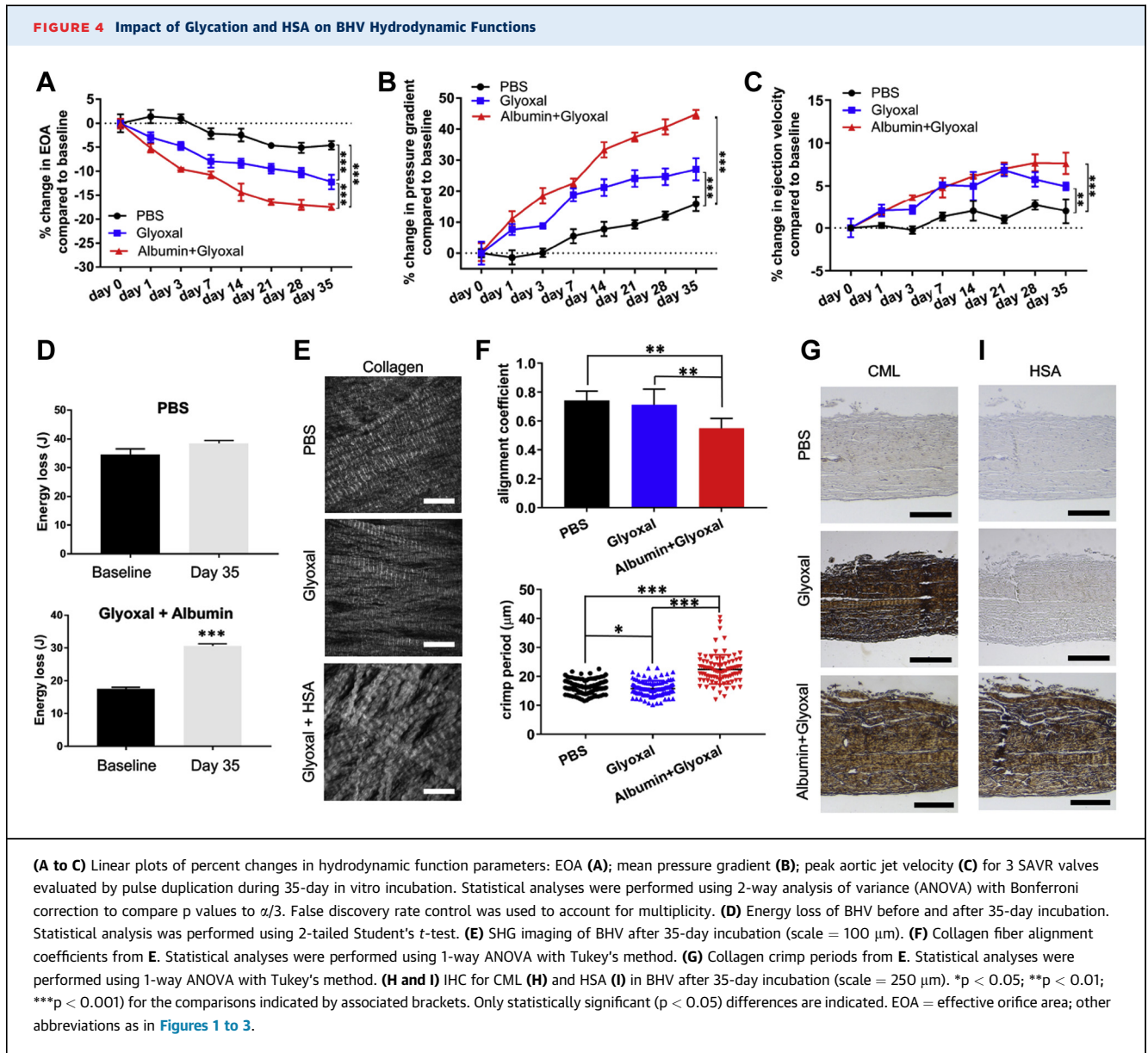
explanted BHVs with various degrees of calcification are shown in **Figures 1C and 1D**. All explanted leaflets, regardless of calcification, showed disruption of collagen alignment by SHG (**Figure 1E**) compared with unimplanted BHVs (**Figure 1B**).

Clinical explants and unimplanted BHV biomaterials (glutaraldehyde-fixed BP and porcine aortic valve) were analyzed by immunohistochemistry (IHC) for generalized AGE, the AGE receptor ligand *N*-carboxymethyl-lysine (CML) (23,24), the AGE cross-link glucosepane (25,26), and HSA (**Figures 1F and 1G**). Each of the 45 SAVR explants exhibited significant IHC staining for glycation products (**Figure 1F**) and HSA (**Figure 1G**) compared with unimplanted BHVs. IHC mean scores for all 45 explants are shown in **Supplemental Figure 1A**. Statistical analysis revealed no relationship of staining intensities to either calcification or the clinical determinants shown, such as diabetes mellitus (**Supplemental Figure 1B**). Collagen malalignment per SHG and positive AGE, CML, HSA, and glucosepane immunostaining were also noted for the TAVR explant (**Supplemental Figure 1C**). In BHV explants fabricated from BP, we observed uniform IHC staining for AGE throughout the tissue, whereas in BHV explants made from porcine aortic valve, IHC exhibited nonuniform staining with significant overlap among glycation products and HSA staining patterns (**Figures 1F and 1G and Supplemental Figures 1D and 1E**).

IN VITRO MODEL OF BHV INTERACTIONS WITH GLYOXAL AND HAS. To investigate the functional mechanisms of glycation and serum protein infiltration, an in vitro model using BP, 50 mmol/l glyoxal as a glycation precursor (12), and a physiological concentration (5% w/v) of clinical-grade serum albumin was designed. IHC on BP following 24 hours of incubation demonstrated glyoxal-generated CML staining and infiltration of HSA uniformly throughout the tissue (**Figure 2A**). Coincubation with glyoxal and HSA yielded increased CML staining compared with glyoxal alone (**Figure 2A**). ^{14}C -glyoxal was used in order to measure the glycation capacity of BP. In a 28-day study, approximately 50% of the incorporated radioactivity seen at 28 days accumulated within the first 24 h (**Figure 2B**). In coincubation, ^{14}C -glyoxal incorporation in BP in the presence of HSA was significantly less than without HSA (**Figure 2B**); however, this diminishment was expected as a result of inherent competition with the solid BP tissue by dissolved human-serum albumin for reaction with glyoxal. Tissue pre-incubated with HSA before incubation in glyoxal alone results in ^{14}C -glyoxal incorporation comparable to the glyoxal-only condition

without correction for any tissue mass increase caused by albumin incorporation. We then sought to visualize whether glycation and HSA infiltration affect the collagen microstructure of BP in vitro. In SHG images, BP samples exposed to either glyoxal or HSA for 28 days demonstrated collagen fiber bundle malalignment and relaxing of crimp compared with BP exposed to PBS. This effect was exacerbated in the presence of both glyoxal and HSA (**Figures 2C and 2D**) and comparable with SHG observations of clinical BHV (**Figure 1E**). To visualize HSA infiltration at the macromolecular level, transmission electron microscopy was performed. Electron micrographs (**Figure 2E**) showed longitudinal and cross-sectional views of collagen fibers from individual fiber bundles. BP incubated in 5% HSA with or without glyoxal exhibited an increase in interfibrillar particulates, whereas incubation with glyoxal alone did not. In addition, interfibrillar particulates appear closely associated with collagen fiber surfaces and demonstrate noncollagen fibrous aggregates in BP coincubated with glyoxal.

RAT SUBCUTANEOUS EXPLANTS AND CIRCULATING BIOMARKERS REVEAL AGE-DEPENDENT CALCIFICATION AND GLYCATION OF BP. An established rat subcutaneous implantation model (**Supplemental Figure 2A**) of BHV calcification was used to investigate glycation in vivo and the impact of animal age in calcification and AGE-mediated SVD (27). Juvenile (3-week-old) and adult (8-month-old) rats received subcutaneous BP implants for either 7 or 30 days. Alizarin red staining (**Figure 3A**) revealed accumulation of calcium deposits within the explants in juvenile animals, which were more extensive in 30-day compared with 7-day explants. No calcification was detectable in adult animals, supporting the clinical observation of age-dependent calcification of BP in vivo (28,29). Quantification of calcium content in BP explants validated this observed increase in calcium accumulation in 30-day ($160 \pm 21.2 \mu\text{g}/\text{mg}$) from 7-day explants ($31.9 \pm 6.8 \mu\text{g}/\text{mg}$), both of which demonstrated greater calcium content compared with unimplanted BP ($0.36 \pm 0.06 \mu\text{g}/\text{mg}$; $p < 0.001$) and to explants from adult animals (**Figure 3B**). Established circulating markers of calcification (PO_4^{4-} [$3.0 \pm 0.19 \mu\text{mol}/\text{ml}$ vs. $2.4 \pm 0.12 \mu\text{mol}/\text{ml}$; $p = 0.028$]; alkaline phosphatase (ALP) [$9.2 \pm 1.5 \text{ mU}/\text{ml}$ vs. $0.30 \pm 0.13 \text{ mU}/\text{ml}$; $p = 0.004$]; and osteopontin (OPN) [$33.9 \pm 3.5 \text{ ng}/\text{ml}$ vs. $9.3 \pm 0.93 \text{ ng}/\text{ml}$; $p < 0.001$]) were also elevated in the plasma of juvenile rats when compared with adult animals (**Figure 3C**). SHG analysis of the rat explants (**Figure 3D**) revealed collagen network disruption in cross sections of both 7- and



30-day BP explants. The alignment coefficients of BP explants were significantly higher in juvenile than in adult animals (0.67 ± 0.02 vs. 0.43 ± 0.02 ; *p* < 0.001) (Figure 3E). In juvenile rats, the 30-day explants demonstrated a higher crimp distance compared with unimplanted BP (28.7 ± 0.40 μ m vs. 25.2 ± 0.45 μ m; *p* < 0.001), indicating the loss of characteristic collagen crimping. Overall, these results indicate progressive and age-dependent glycation and concomitant structural disruption of collagen alignment in BP tissue in the rat model. IHC (Figure 3F) revealed diffuse CML accumulation within both the 7- and 30-day BP explants that was more prominent in the juvenile animals. Plasma concentrations

(Figure 3G) of soluble receptor for AGE (sRAGE) (3.7 ± 0.47 ng/ml vs. 1.7 ± 0.30 ng/ml; *p* = 0.007), methylglyoxal (3.9 ± 0.88 nmol/l vs. 1.3 ± 0.34 nmol/l; *p* = 0.020), and methylglyoxal protein adducts (6.8 ± 0.76 μ g/ml vs. 1.3 ± 0.19 μ g/ml; *p* < 0.001) were all increased in the juvenile rats compared with the adult cohort. IHC using an anti-HSA antibody (Figure 3H) that cross-reacts with rat albumin also indicated infiltration of albumin throughout the BP tissue by 7 days, with enhanced accumulation after 30 days. In contrast to all other plasma marker analyses, the plasma concentration of glycated albumin (Figure 3I) was lower in the juvenile rats (325 ± 45.3 pmol/ml) compared with the adult cohort (539 ± 35.4 pmol/ml);

$p = 0.006$). IHC also revealed diffuse staining for OPN (Supplemental Figure 2B) and AGE (Supplemental Figure 2C) in both 7- and 30-day implants, which was more pronounced in the juvenile animals. IHC for RAGE (Supplemental Figure 2D) demonstrated positive staining at the surface of 7- and 30-day explants from both juvenile and adult rats. IHC studies did not detect the presence of glucosepane in the subcutaneous explants (data not shown).

IMPACT OF AGE ACCUMULATION ON BIOPROSTHETIC VALVE HYDRODYNAMIC PERFORMANCE.

To understand the susceptibility of intact BHV leaflets to glycation and HSA infiltration as well as to determine the roles of these mechanisms in degeneration of valve performances, we incubated 3 expired clinical-grade Carpentier-Edwards PERIMOUNT RSR BHVs (Edwards Lifesciences, Irvine, California) in PBS, 50 mmol/l glyoxal in PBS, and 50 mmol/l glyoxal plus 5% HSA in PBS, respectively, at 37°C for 35 days and evaluated their hydrodynamic function under physiological conditions. Hydrodynamic function of the valves was tested at 0, 1, 3, 7, 14, 21, 28, and 35 days of incubation using an ISO standard heart valve pulse duplicator system (test conditions in Supplemental Appendix). The baseline (time point “0”) values of mean pressure gradient and effective orifice area (EOA) of all 3 valves satisfied the requirements specified in ISO-5840, indicating the expected hydrodynamic performances of SAVR valves used in this study (Figures 4A to 4C). Both experimental in vitro incubation conditions resulted in a steady decline in EOA (Figures 4A to 4C) and increases in mean pressure gradient and peak jet velocity over time. Following 35 days of in vitro treatment, the BHV coincubated with glyoxal and HSA demonstrated a 17.5% decrease in EOA, 44.9% increase in mean pressure gradient, and 7.6% increase in peak jet velocity as compared with each of the baseline values. The BHV treated with glyoxal alone showed a 12.3% decrease in EOA, 27.1% increase in mean pressure gradient, and 5.0% increase in peak jet velocity as compared with its baseline values (Figures 4A to 4C). By comparison, the BHV incubated in PBS alone exhibited 4.6%, 15.9%, and 2.0% changes in these 3 parameters, respectively (Figures 4A to 4C and Supplemental Figure 3, Supplemental Table 2). Energy loss during each cycle was not significantly changed after 35-day PBS incubation (Figure 4D); however, glyoxal and HSA coincubation resulted in significantly worsened energy loss after 35 days (17.5 ± 0.23 J [baseline] vs. 30.6 ± 0.35 J [day 35]; $p < 0.001$) (Figure 4D). SHG imaging (Figure 4E) and analysis (Figures 4F and 4G) of valve leaflets after 35 days of treatments revealed collagen

malalignment and the relaxation of collagen crimp following coincubated with glyoxal and HSA as compared with PBS or glyoxal. Similar to BP glycated in vitro, leaflet tissue of the valve treated with glyoxal alone was positively stained for CML, whereas the valve coincubated in glyoxal and HSA demonstrated leaflet accumulation of CML and HSA (Figures 4H and 4I). We investigated the significance of glycation and concomitant HSA infiltration to TAVR functionality using an in-house fabricated TAVR valve (Supplemental Figure 4A). Valve fabrication is described in the Supplemental Appendix. Similar to the observations in SAVR valves, TAVR valve also demonstrated collagen malalignment, decline in EOA, and increases in mean pressure gradient, peak jet velocity, and energy loss (Supplemental Figures 4B to 4G, Supplemental Table 2) as a result of coincubation with glyoxal and HSA. IHC assessments of HSA, AGE, and CML in our fabricated TAVR valve (Supplemental Figure 4C) showed similar results to those in clinical explants as well as our in vitro and in vivo studies.

DISCUSSION

Glycation is well-established as a functional mechanism of tissue degeneration in various diseases (13), yet this study is the first description of its involvement in the degeneration of BHVs. Similarly, whereas infiltration of circulating proteins on or in clinical (30-32) and in vivo (33,34) BHV tissue has been reported, this work establishes the relevance of serum albumin infiltration as well as interaction between protein infiltration and glycation in affecting BHV hydrodynamic performances. Our study employed a comprehensively translational approach, establishing clinical relevance via explant analyses (Figure 1), performing mechanistic modeling in vitro (Figure 2) and in vivo (Figure 3), and evaluating the functional significance of the mechanisms using a cardiac simulator (Figure 4).

IHC on 45 clinical explants indicate that accumulations of AGEs and HSA are prevalent in failed BHVs and show collagen malalignment independently of the extent of calcification. The accumulation of AGEs and HSA, together with the general lack of correlation with calcification, valve tissue type, or diabetes, suggest that glycation and albumin infiltration are fundamental mechanisms affecting all implanted BHVs. Although diabetes is logically expected to exacerbate glycation, we may have not been able to discern enhancement of glycation in a subpopulation of our failed valves, due to our IHC results indicating potentially saturated staining in general. Diabetes

may instigate earlier achievement of these high levels of glycation. Diabetic patient valves did tend to fail earlier (6.9 ± 2.1 years) than nondiabetic valves (9.0 ± 2.7 years) in our cohort, which skews toward early failures overall (8.6 ± 2.7 years). Our findings provide a mechanistic rationale explaining recent observations that SVD tends to occur earlier and more commonly in diabetic patients (4), who had glycation-related pathologies are highly exacerbated. Our results also inform understanding of the complex relationship between atherosclerosis-related changes and calcification in BHV. Atherosclerotic risk factors have been associated with SVD and atherosclerosis-like processes, such as lipid infiltration and inflammatory cell activation, are known to occur in BHV (3,7). Conflicting results have been reported regarding the effects of statin treatment on SVD and BHV calcification (35-37). Calcification has also been related to deposition of calcium-binding proteins in BHV. Although the protein deposition process generally involves endothelial barrier dysfunction and inflammatory cell-mediated events in atherosclerosis, the results reported here for albumin suggest that calcification-related protein deposition in BHV may be an atherosclerosis-unrelated, cell-free diffusive infiltration event. Nonetheless, glycation—particularly via glycated albumin—is also known to play roles in atherosclerosis-related processes via inflammatory cell activation (11,13,14). It is therefore reasonable to expect that glycation contributes to established inflammatory processes that occur on and in BHV. The experimental paradigms and hypotheses reported here provide a platform for further studies into the complex interactions of these mechanisms and cofactors in BHV SVD, which may explain the underpinnings of SVD in particular patient populations.

We sought to understand the mechanisms of AGE and HSA accumulation in BHVs by a glycation/protein infiltration *in vitro* model. The observed accumulation of AGEs and HSA throughout BP tissue after only 24 h of *in vitro* incubation implies that these processes begin impinging on BHV immediately upon implantation. Together, clinical correlation and *in vitro* assays suggest that HSA incorporation is enabled by glycation and/or that incorporated HSA increases the tissue's capacity for glycation. The former possibility is supported by published data suggesting that glycation crosslinking permanently incorporates infiltrated albumin into solid tissue matrices (38-40). The latter possibility is informed by our clinical *ex vivo* and *in vitro* modeling observations, indicating preferential accumulation of glycation products at areas of HSA incorporation in clinical BHV and enhancement of tissue CML accumulation amid diminished overall

glycation due to glyoxal exposure by coincubation with HSA. Glycation occurs primarily on lysine and arginine residues, while the majority of BHV tissue lysines are effectively sequestered from glycation by prior reaction with glutaraldehyde. Incorporation of infiltrated proteins, whose residues are generally unmodified, would increase the repository of glycation-susceptible lysines—as well as arginines—in the tissue. These observations suggest that human-derived serum albumin infiltration not only exacerbates accumulation of AGE in BHV, but also modifies the glycation profile toward lysine-directed AGE, which include the most prominent signaling AGE, CML (14,23,24), and the most abundant crosslinking AGE, glucosepane (25,26). Thus, the mechanistic crosstalk between glycation and HSA coincubation lead to the highest degree of structural alteration by SHG assessment and electron microscopy. Additionally, the incorporation of proteins may inculcate BHV tissue with the properties of those proteins, such as calcium- and lipid-binding as well as high oncotic pressure in the case of HSA.

The rat model is an established method for testing biomaterial properties and calcification *in vivo*. This model resulted in calcium phosphate deposition within the central region of BP tissue (comparable to observations in clinical explants [41]), rather than on the surface, as noted with *in vitro* calcium-phosphate incubations (42). This system also allows modeling major risk factors for BHV failure, such as patient age. The assessments of both explants and circulating markers indicate a host-age dependence of tissue glycation, suggesting that enhanced glycation as well as calcification could contribute to accelerated SVD in pediatric patients. sRAGE derived from inflammatory cell turnover has been studied as a biomarker for cardiovascular disorders. RAGE is expressed on monocyte cell membranes, and RAGE ligand (such as CML) signaling can initiate monocyte-to-macrophage transition. Inflammatory cell aggregates in BHVs tend to be surface oriented, which is reflected by the hematoxylin counterstain of rat explants. It is possible that AGE formation in BHVs provides the opportunity for RAGE signaling and macrophage deposition to produce reactive oxygen species that result in OxAA formation in BHV, as we demonstrated in both experimental and clinical BHV studies (8,43). The lack of demonstrable glucosepane in the rat explants may be due to short (30-day) implantation times.

Cardiac pulse simulators are required for hydrodynamic performance analysis of prosthetic heart valves under ISO 5840 standard and the U.S. Food and Drug Administration guidance. Thus, we aimed to provide functional evidence that AGE and HSA

accumulation weaken hydrodynamic performances of BHVs upon *in vitro* glycation. EOA, mean pressure gradient, and peak aortic jet velocity, were calculated to assess the hydrodynamic performances of BHV. All 3 parameters are important indicators for the clinical assessment of aortic valve stenosis severity (44,45). All *in vitro* incubation conditions resulted in a steady decline in EOA and increases in mean pressure gradients and peak jet velocities. These results suggest that the generation of AGEs in BHV significantly alters the biomechanical properties of valve leaflets, potentially causing leaflet stiffening. Additionally, BHV treated with glyoxal alone demonstrated less deterioration of hydrodynamic performances as compared with glyoxal and HSA coincubation. This could be attributed to the fact that HSA provides additional reactive sites for glyoxal and enhances AGE formation. Deterioration of hydrodynamic function in the forms of increased pressure gradients and jet velocities as well as decreased EOA is a definitive feature of the SVD pipeline and its diagnosis (3,46). Together, the ubiquity of glycation product as well as serum albumin accumulation in failed clinical BHV and the demonstration of the sufficiency of glycation and concomitant albumin infiltration to degenerate BHV hemodynamic properties indicate that these synergistic mechanisms may be core elements driving noncalcific SVD in all BHV patients and in diabetic patients in particular (4).

STUDY LIMITATIONS. Our clinical series included only aortic valve replacements. Nevertheless, SVD mechanisms are comparable regardless of implant site (47,48). We restricted our study to a small group of representative glycation-related structures. AGE research has identified a myriad of moieties including numerous crosslinks and receptor ligands (11,12). The HSA used in our *in vivo* studies is a clinical grade, human isolated HSA to closely mimic *in vivo* albumin conditions. Assessing SVD in rat subcutaneous implants that lack exposure to systemic blood flow may be a critical consideration; however, our data show that HSA permeated throughout the implanted BP as in clinical BHV explants. There are also some limitations on our pulse duplicator assays including: 1) using physiological buffers rather than blood or fluids with viscosity approximating that of blood; and 2) the use of clinical BHVs with expired shelf-life dates, per Food and Drug Administration requirements, that could alter their susceptibility to glycation. However, the baseline hydrodynamic performances met the ISO-5840 standards. It should also be noted that the present studies did not include experiments involving inhibition of glycation, or the use of so-called “AGE-breakers” that have been shown to

diminish AGE accumulation experimentally. These studies were not considered because none of the agents previously studied have been shown to be effective in clinical trials, and there are no approved antiglycation agents available for clinical use.

CONCLUSIONS

Overall, SVD is a multifactorial process that involves far more than the passive degeneration of leaflet materials. We propose that glycation and protein infiltration result in BHV tissue matrix disruption via multiple mechanisms: 1) reduction of BHV leaflet mechanical compliance due to AGE crosslinking; 2) enabling of the permanent incorporation of infiltrated proteins via AGE crosslinking (38-40); 3) modification of BHV leaflets by AGE and protein incorporation that can alter collagen fiber interactions and resultant force dissipation during biomechanical activity (16-18); and 4) proinflammatory responses to the valve leaflet tissue by signaling to receptors of glycation products, including the receptor for AGE (RAGE) (14,15,24). Thus, it is concluded that the accumulation of AGE and serum albumin in clinical explants and the impact of glycation on both the collagen fiber microstructure and on the hydrodynamic function of BHVs significantly contribute to SVD. Interactions of these mechanisms with other mechanisms and cofactors involved in SVD are being evaluated and will be reported in subsequent papers.

ADDRESS FOR CORRESPONDENCE: Dr. Giovanni Ferrari, Departments of Surgery and Biomedical Engineering, Columbia University, 630 West 168th Street, 17.413, New York, New York 10032. E-mail: gf2375@cumc.columbia.edu.

PERSPECTIVES

COMPETENCY IN MEDICAL KNOWLEDGE:

Advanced glycation end products together with serum protein infiltration are well-established contributors to diabetes and Alzheimer's disease, and many other disorders. The association of this pathophysiology with bioprosthetic heart valve structural degeneration represents a novel disease mechanism that should be recognized and addressed.

TRANSLATIONAL OUTLOOK:

Future clinical studies can identify high risk populations and study interventions to reduce the deleterious impact of advanced glycation end products and serum protein infiltration on bioprosthetic heart valve functionality.

REFERENCES

1. Head SJ, Celik M, Kappetein AP. Mechanical versus bioprosthetic aortic valve replacement. *Eur Heart J* 2017;38:2183-91.
2. Isaacs AJ, Shuhaiber J, Salemi A, Isom OW, Sedrakyan A. National trends in utilization and in-hospital outcomes of mechanical versus bioprosthetic aortic valve replacements. *J Thorac Cardiovasc Surg* 2015;149:1262-9.e3.
3. Dvir D, Bourguignon T, Otto CM, et al. Standardized definition of structural valve degeneration for surgical and transcatheter bioprosthetic aortic valves. *Circulation* 2018;137:388-99.
4. Lorusso R, Gelsomino S, Luca F, et al. Type 2 diabetes mellitus is associated with faster degeneration of bioprosthetic valve: results from a propensity score-matched Italian multicenter study. *Circulation* 2012;125:604-14.
5. Saleeb SF, Gauvreau K, Mayer JE, Newburger JW. Aortic valve replacement with bovine pericardial tissue valve in children and young adults. *Circulation* 2019;139:983-5.
6. Li KYC. Bioprosthetic heart valves: upgrading a 50-year old technology. *Front Cardiovasc Med* 2019;6:47.
7. Rodriguez-Gabella T, Voisine P, Puri R, Pibarot P, Rodes-Cabau J. Aortic bioprosthetic valve durability: incidence, mechanisms, predictors, and management of surgical and transcatheter valve degeneration. *J Am Coll Cardiol* 2017;70:1013-28.
8. Lee S, Levy RJ, Christian AJ, et al. Calcification and oxidative modifications are associated with progressive bioprosthetic heart valve dysfunction. *J Am Heart Assoc* 2017;6:e005648.
9. Roselli EE, Smedira NG, Blackstone EH. Failure modes of the Carpentier-Edwards pericardial bioprosthesis in the aortic position. *J Heart Valve Dis* 2006;15:421-7. discussion 427-8.
10. Salaun E, Clavel MA, Rodes-Cabau J, Pibarot P. Bioprosthetic aortic valve durability in the era of transcatheter aortic valve implantation. *Heart* 2018;104:1323-32.
11. Ott C, Jacobs K, Haucke E, Navarrete Santos A, Grune T, Simm A. Role of advanced glycation end products in cellular signaling. *Redox Biol* 2014;2: 411-29.
12. Vistoli G, De Maddis D, Cipak A, Zarkovic N, Carini M, Aldini G. Advanced glycoxidation and lipoxidation end products (AGEs and ALEs): an overview of their mechanisms of formation. *Free Radical Res* 2013;47:3-27.
13. Singh R, Barden A, Mori T, Beilin L. Advanced glycation end-products: a review. *Diabetologia* 2001;44:129-46.
14. Basta G, Schmidt AM, De Caterina R. Advanced glycation end products and vascular inflammation: implications for accelerated atherosclerosis in diabetes. *Cardiovasc Res* 2004; 63:582-92.
15. Gkogkolou P, Bohm M. Advanced glycation end products: key players in skin aging? *Derma-toendocrinol* 2012;4:259-70.
16. Fessel G, Li Y, Diederich V, et al. Advanced glycation end-products reduce collagen molecular sliding to affect collagen fibril damage mechanisms but not stiffness. *PLoS One* 2014;9: e110948.
17. Gautieri A, Passini FS, Silvan U, et al. Advanced glycation end-products: mechanics of aged collagen from molecule to tissue. *Matrix Biol* 2017; 59:95-108.
18. Paul RG, Bailey AJ. Glycation of collagen: the basis of its central role in the late complications of ageing and diabetes. *Int J Biochem Cell Biol* 1996; 28:1297-310.
19. Schoen FJ, Tsao JW, Levy RJ. Calcification of bovine pericardium used in cardiac valve bioprostheses. Implications for the mechanisms of bioprosthetic tissue mineralization. *Am J Pathol* 1986;123:134-45.
20. Soares JS, Feaver KR, Zhang W, Kamensky D, Aggarwal A, Sacks MS. Biomechanical behavior of bioprosthetic heart valve heterograft tissues: characterization, simulation, and performance. *Cardiovasc Eng Technol* 2016;7:309-51.
21. Cohen MP. Intervention strategies to prevent pathogenetic effects of glycated albumin. *Arch Biochem Biophys* 2003;419:25-30.
22. Gil H, Salcedo D, Romero R. Effect of phosphate buffer on the kinetics of glycation of proteins. *J Phys Org Chem* 2005;18:183-6.
23. Delgado-Andrade C. Carboxymethyl-lysine: thirty years of investigation in the field of AGE formation. *Food Funct* 2016;7:46-57.
24. Kislinger T, Fu C, Huber B, et al. N(epsilon)-(carboxymethyl)lysine adducts of proteins are ligands for receptor for advanced glycation end products that activate cell signaling pathways and modulate gene expression. *J Biol Chem* 1999;274: 31740-9.
25. Sjoberg JS, Bulterijs S. Characteristics, formation, and pathophysiology of glucosepane: a major protein cross-link. *Rejuvenation Res* 2009;12: 137-48.
26. Monnier VM, Sun W, Sell DR, Fan X, Nemet I, Genuth S. Glucosepane: a poorly understood advanced glycation end product of growing importance for diabetes and its complications. *Clin Chem Lab Med* 2014;52:21-32.
27. Bonetti A, Marchini M, Ortolani F. Ectopic mineralization in heart valves: new insights from in vivo and in vitro procalcific models and promising perspectives on noncalcifiable bioengineered valves. *J Thorac Dis* 2019;11:2126-43.
28. Saleeb SF, Newburger JW, Geva T, et al. Accelerated degeneration of a bovine pericardial bioprosthetic aortic valve in children and young adults. *Circulation* 2014;130:51-60.
29. Etnel JR, Elmont LC, Ertekin E, et al. Outcome after aortic valve replacement in children: A systematic review and meta-analysis. *J Thorac Cardiovasc Surg* 2016;151:143-52.e1-3.
30. Shen M, Marie P, Farge D, et al. Osteopontin is associated with bioprosthetic heart valve calcification in humans. *C R Acad Sci III* 1997;320:49-57.
31. Shen M, Carpentier SM, Berrebi AJ, Chen L, Martinet B, Carpentier A. Protein adsorption of calcified and noncalcified valvular bioprostheses after human implantation. *Ann Thorac Surg* 2001; 71 Suppl:5406-7.
32. Sakaue T, Nakaoka H, Shikata F, et al. Biochemical and histological evidence of deteriorated bioprosthetic valve leaflets: the accumulation of fibrinogen and plasminogen. *Biol Open* 2018;7:bio034009.
33. Levy RJ, Schoen FJ, Levy JT, Nelson AC, Howard SL, Oshry LJ. Biologic determinants of dystrophic calcification and osteocalcin deposition in glutaraldehyde-preserved porcine aortic valve leaflets implanted subcutaneously in rats. *Am J Pathol* 1983;113:143-55.
34. Levy RJ, Zenker JA, Bernhard WF. Porcine bioprosthetic valve calcification in bovine left ventricle-aorta shunts: studies of the deposition of vitamin K-dependent proteins. *Ann Thorac Surg* 1983;36:187-92.
35. Lee S, Kim DH, Youn YN, Joo HC, Yoo KJ, Lee SH. Rosuvastatin attenuates bioprosthetic heart valve calcification. *J Thorac Cardiovasc Surg* 2019;158:731-41.e1.
36. Gilmanov D, Bevilacqua S, Mazzone A, Glauber M. Do statins slow the process of calcification of aortic tissue valves? *Interact Cardiovasc Thorac Surg* 2010;11:297-301.
37. Antonini-Canterin F, Zuppiroli A, Popescu BA, et al. Effect of statins on the progression of bioprosthetic aortic valve degeneration. *Am J Cardiol* 2003;92:1479-82.
38. Yamaji T, Fukuhara T, Kinoshita M. Increased capillary permeability to albumin in diabetic rat myocardium. *Circ Res* 1993;72:947-57.
39. Londono I, Leclerc Y, Bendayan M. Ultrastructural localization of endogenous albumin in human aortic tissue by protein A-gold immunocytochemistry. *Am J Pathol* 1992;140: 179-91.
40. Sajithlal GB, Chithra P, Chandrakasan G. Advanced glycation end products induce cross-linking of collagen in vitro. *Biochim Biophys Acta* 1998;1407:215-24.
41. Schoen FJ, Levy RJ. Bioprosthetic heart valve failure: pathology and pathogenesis. *Cardiol Clin* 1984;2:717-39.
42. Abolhoda A, Yu S, Oyarzun JR, McCormick JR, Bogden JD, Gabbay S. Calcification of bovine pericardium: glutaraldehyde versus No-React biomodification. *Ann Thorac Surg* 1996;62:169-74.

43. Christian AJ, Alferiev IS, Connolly JM, Ischiropoulos H, Levy RJ. The effects of the covalent attachment of 3-(4-hydroxy-3,5-di-tert-butylphenyl) propyl amine to glutaraldehyde pretreated bovine pericardium on structural degeneration, oxidative modification, and calcification of rat subdermal implants. *J Biomed Mater Res A* 2015;103:2441-8.
44. Saikrishnan N, Kumar G, Sawaya FJ, Lerakis S, Yoganathan AP. Accurate assessment of aortic stenosis: a review of diagnostic modalities and hemodynamics. *Circulation* 2014; 129:244-53.
45. Baumgartner H, Hung J, Bermejo J, et al. Recommendations on the echocardiographic assessment of aortic valve stenosis: a focused update from the European Association of Cardiovascular Imaging and the American Society of Echocardiography. *J Am Soc Echocardiogr* 2017; 30:372-92.
46. Salaun E, Mahjoub H, Dahou A, et al. Hemodynamic deterioration of surgically implanted bioprosthetic aortic valves. *J Am Coll Cardiol* 2018;72:241-51.
47. Pibarot P, Dumesnil JG. Prosthetic heart valves: selection of the optimal prosthesis and long-term management. *Circulation* 2009;119:1034-48.
48. Paradis JM, Del Trigo M, Puri R, Rodes-Cabau J. Transcatheter valve-in-valve and valve-in-ring for treating aortic and mitral surgical prosthetic dysfunction. *J Am Coll Cardiol* 2015;66: 2019-37.

KEY WORDS advanced glycation end products, aortic valve disease, biomaterial, bioprosthetic heart valve

APPENDIX For an expanded Methods section and supplemental figures and tables, please see the online version of this paper.